

## NMR study of $U(\text{Be}, \text{B})_{13}$ in the normal and superconducting states

E. T. Ahrens,\* R. H. Heffner, P. C. Hammel, A. P. Reyes,† J. D. Thompson, and J. L. Smith  
*Los Alamos National Laboratory, Los Alamos, New Mexico 87545*

W. G. Clark

*Department of Physics and Astronomy, University of California, Los Angeles, California 90095-1547*

(Received 1 July 1998)

We report extensive  $^{11}\text{B}$  and  $^9\text{Be}$  nuclear magnetic resonance (NMR) spin-lattice relaxation time ( $T_1$ ) and Knight shift measurements in the heavy-fermion superconductor  $U\text{Be}_{13-x}\text{B}_x$  ( $x=0.030, 0.067$ ). Data were acquired over a broad temperature ( $T$ ) range spanning 0.096–300 K in both the normal and superconducting states. In the normal state, the  $^{11}\text{B}$   $T$  dependence of  $T_1$  displayed several energy scales. In a narrow  $T$  range, between 1 and 2 K,  $1/T_1 T$  was roughly constant. At lower temperatures and in a magnetic field exceeding the upper critical field,  $1/T_1 T$  exhibited a monotonic decrease down to approximately 0.18 K. Above roughly 4 K,  $1/T_1$  exhibited a weak  $T$  dependence until  $\sim 60$  K. At higher temperatures, additional relaxation mechanisms were present. The  $1/T_1$  values for both  $^9\text{Be}$  and  $^{11}\text{B}$  for all B concentrations were indistinguishable above  $\sim 4$  K; however, at temperatures of the order of 1 K, the  $x=0.067$  sample had values roughly twice that of the  $x=0.030$  sample for either nuclei. The  $x=0.030$  sample had essentially the same  $1/T_1$  magnitude and  $T$  dependence as undoped  $U\text{Be}_{13}$ . From the linear plot of the Knight shift ( $K_B$ ) versus the static magnetic susceptibility ( $\chi$ ), the  $^{11}\text{B}$  hyperfine field coupling constant was calculated to be  $-361.1 \text{ Oe}/\mu_B$ . An approximate analysis of the U moment electronic fluctuation rate ( $\Gamma$ ) was performed using the measured values of  $1/T_1$ ,  $K_B$ , and  $\chi$ . We observed a  $\Gamma \propto \sqrt{T}$  dependence between 8 and 70 K, which is consistent with the existence of isolated local moment fluctuations. For  $T > 70$  K, the  $\Gamma$  analysis breaks down due to the presence of crystal field excitations. Measurements of  $1/T_1$  indicated a moderate decrease in  $\Gamma$  with the addition of boron at low temperatures, where  $\Gamma(x=0.030)/\Gamma(x=0.067) \approx 2$ . At lower temperatures,  $\Gamma$  approached a constant value of the order of 1 meV at  $T \approx 2$  K. In the superconducting state, the  $T$  dependence of  $1/T_1$  exhibited an absence of power-law behavior and a strong B concentration dependence for both nuclei. This behavior is consistent with gapless superconductivity induced by the B impurities. The ratio of the  $^9\text{Be}$  to  $^{11}\text{B}$   $1/T_1$  increased with decreasing  $T$  below  $T_c$ . This indicates additional contributions to the  $^9\text{Be}$   $1/T_1$  at low temperatures that we attribute to spin diffusion processes that have negligible impact on the dilute  $^{11}\text{B}$ . Below  $T_c$ , the  $^{11}\text{B}$  Knight shift was measured to be  $-0.08 (\pm 0.01)\%$  and was independent of both  $x$  and  $T$ .  
 [S0163-1829(99)03602-4]

### I. INTRODUCTION

The superconducting properties of heavy-fermion materials are extremely sensitive to the substitution of chemical impurities regardless of whether or not the dopant possesses a magnetic moment. In  $U\text{Be}_{13}$ , a few tenths of a percent of Cu substituted for Be completely eliminates its superconductivity.<sup>1</sup> Most impurities depress the superconducting transition temperature ( $T_c$ ) presumably due to pair breaking. Other dopants, such as Th-alloyed  $U\text{Be}_{13}$ , can induce multiple superconducting phases<sup>2</sup> and provide insight into the exotic nature of the superconducting state. Boron substituted for Be is another case that results in a remarkable change in the superconducting properties.<sup>3</sup> Some of these changes include (i) a large enhancement in the specific heat discontinuity  $\Delta C$  at  $T_c$ , which can reach values nearly twice that of pure  $U\text{Be}_{13}$  and exceeds the Bardeen-Cooper-Schrieffer theoretical value by a wide margin,<sup>3</sup> (ii) a relatively small depression of  $T_c$  with B doping, which is in sharp contrast to the behavior of other nonmagnetic impurities (e.g., Cu) added at comparable doping levels, and (iii) evidence for a reduction in the coherence temperature<sup>4</sup>  $T^*$  with increasing B concentration.<sup>5</sup>

In this paper we report results of a nuclear magnetic resonance (NMR) investigation into the peculiar behavior of  $U\text{Be}_{13-x}\text{B}_x$ . In this system, as in many other heavy fermions, many of the low-temperature thermodynamic properties can be interpreted as resulting from a narrow feature in the density of states in proximity to the Fermi energy that is presumably due to low-energy magnetic fluctuations. NMR is well suited to probe this low-energy response because of the weak coupling of the nuclei to the metallic environment and the exceedingly small energy carried by the Larmor frequency photon.

We describe measurements of the spin-lattice relaxation time ( $T_1$ ) and the Knight shift ( $K_B$ ) in  $U\text{Be}_{13-x}\text{B}_x$  for  $x = 0.030$  and  $0.067$  at temperatures ( $T$ ) ranging from 0.096 to 300 K. Both the  $^9\text{Be}$  and  $^{11}\text{B}$  signals were investigated. In the normal state,  $^{11}\text{B}$  measurements were made between 0.192 and 300 K. At the lowest temperatures, we applied a magnetic field exceeding the upper critical field ( $H_{c2}$ ). The  $^{11}\text{B}$  NMR signal is particularly useful because its spectrum exhibits a relatively narrow, symmetric line shape, as shown in Fig. 1. Consequently, the resonance position can be accurately determined for Knight shift measurements. We have

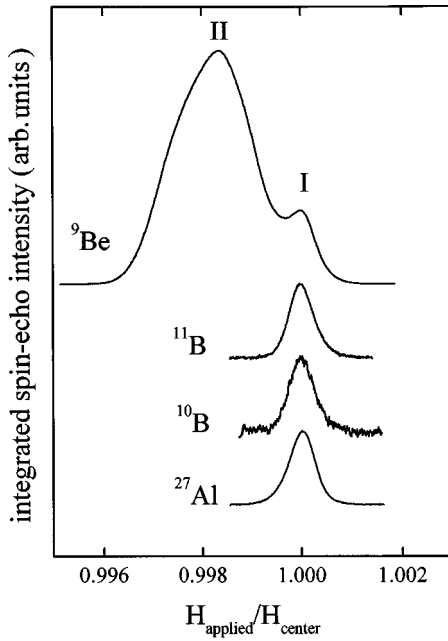


FIG. 1. Spectra of  ${}^9\text{Be}$ ,  ${}^{11}\text{B}$ ,  ${}^{10}\text{B}$ , and  ${}^{27}\text{Al}$  in the  $x=0.030$  sample taken at 4 K. (The Al is mixed into the powdered sample as a local field reference.) The labels I and II denote the approximate positions of the inequivalent Be(I) and Be(II) site locations. For each spectra, the field axis is normalized to the centroid field position, except for the  ${}^9\text{Be}$  spectrum, which is normalized to the approximate position of the Be(I) feature. The spectral linewidth is field dependent (Ref. 6) and is virtually temperature independent (at constant field) from  $\sim 2$  K down to the lowest temperatures investigated. The B dopant resides exclusively on the  $m3$  or cubic Be(I) site of the  $\text{UBe}_{13}$  lattice (Ref. 6). The Be(II) site has lower symmetry. The  ${}^{11}\text{B}$  signal is particularly useful because its spectrum exhibits a relatively narrow, symmetric, line shape, which permits accurate Knight shift measurements. The spectra were taken at spectrometer frequencies of 52 MHz for  ${}^9\text{Be}$  and  ${}^{10}\text{B}$  and 95 and 63 MHz for  ${}^{11}\text{B}$  and  ${}^{27}\text{Al}$ , respectively. These spectra were measured using conventional spin-echo spectroscopy, where the height of the echo was monitored using a gated boxcar integrator as the field was swept through the resonance.

previously shown that the B dopant resides exclusively in the  $m3$  or cubic Be(I) site of the  $\text{UBe}_{13}$  lattice.<sup>6</sup> The inequivalent Be(II) site has lower symmetry. A preliminary account of the  $T_1$  results in the superconducting state has been presented earlier.<sup>7</sup>

Our results show that in the normal state, the  $T$  dependence of the magnetic response probed by  $1/T_1$  displays several energy scales. At low temperatures,  $1/T_1 T$  was roughly constant over a narrow temperature range of roughly 1 to 2 K; below these temperatures  $1/T_1 T$  exhibited a monotonic decrease down to the lowest temperature investigated. Above approximately 4 K,  $1/T_1$  exhibited a weak temperature dependence until  $\sim 60$  K. At higher temperatures, additional relaxation mechanisms were present, presumably due to low-lying crystal field excitations.

The  ${}^{11}\text{B}$  hyperfine field coupling constant was extracted from a plot of the measured  $K_B$  as a function of the static magnetic susceptibility ( $\chi$ ). From the measured hyperfine field  $T_1$  and  $\chi$ , we estimated the  $T$  dependence of the electronic fluctuation rate ( $\Gamma$ ) associated with the U moments.

In the superconducting state ( $T_c \sim 0.8$  K), we investigated the  $T$  dependence of  $T_1$  for both the  ${}^9\text{Be}$  and  ${}^{11}\text{B}$  nuclei. Below  $T_c$ ,  $1/T_1$  exhibited a strong B concentration dependence, especially at the lowest temperatures. We interpret this behavior as consistent with gapless superconductivity induced by the B impurities. The ratio of the  ${}^9\text{Be}$  to  ${}^{11}\text{B}$   $1/T_1$  increased with decreasing temperature below  $T_c$ . This observation indicates that there are additional contributions to the  ${}^9\text{Be}$  relaxation rate that we attribute to processes involving nuclear spin diffusion that are less effective at relaxing the dilute  ${}^{11}\text{B}$ . Below  $T_c$ , the  ${}^{11}\text{B}$  Knight shift was independent of  $x$  and  $T$  within experimental uncertainties.

There are several previous studies utilizing  ${}^9\text{Be}$  NMR to investigate pure and alloyed  $\text{UBe}_{13}$ .<sup>8–12</sup> MacLaughlin *et al.*<sup>8</sup> investigated  $\text{U}_{1-x}\text{Th}_x\text{Be}_{13}$  ( $x=0$  and 0.033) in the superconducting state. An approximate  $1/T_1 \propto T^3$  dependence was observed well below  $T_c$ , suggesting an anisotropic superconducting gap and an unconventional pairing mechanism. In the normal state,  $1/T_1 T \sim \text{const}$  was observed in a narrow temperature range just above  $T_c$ . Clark *et al.*<sup>10,11</sup> investigated the normal state Knight shift and quadrupolar interactions in single-crystal  $\text{UBe}_{13}$  (Ref. 10) and high-temperature ( $T < 1000$  K)  $T_1$  behavior in powdered samples.<sup>11</sup> Also, normal state electronic spin fluctuation rates have been studied in the undoped material.<sup>12</sup>

## II. EXPERIMENTAL DETAILS

Polycrystalline samples of  $\text{UBe}_{13-x}\text{B}_x$  for  $x=0.030$  and 0.067 were prepared using standard arc melting techniques. For each concentration, powdered samples with particle diameters ranging from 38 to 128  $\mu\text{m}$  were prepared. For both samples,  $T_c \approx 0.9$  K and varied by less than 15% between samples.<sup>5</sup> To confirm that the B concentrations were equal to the nominal values, we measured the ratio of  ${}^{11}\text{B}$  to  ${}^9\text{Be}$  nuclei in each sample using the intensity of their NMR signals. From this ratio, the B concentrations were calculated and they agreed with the nominal values to better than 12%. This measurement confirmed that the observed  ${}^{11}\text{B}$  resonance originated from a single phase containing all of the dopant. The  $\text{UBe}_{13-x}\text{B}_x$  samples used in this NMR study were the same ones used in resistivity, magnetic susceptibility, specific heat, and muon spin relaxation ( $\mu\text{SR}$ ) experiments.<sup>5</sup>

Within the temperature range between 2 and 300 K, sample cooling was achieved using a commercial helium gas-flow cryostat. It was mounted inside a 9-T magnet connected to a variable current supply. Powdered samples ( $\sim 250$  mg) were loosely packed into cylindrical tubes that were surrounded by a copper solenoid. A conventional laboratory-built wideband pulsed NMR spectrometer was used for all measurements.

A laboratory-built dilution refrigerator was used for sample cooling below 2 K. The experimental samples, NMR coils, and resistance thermometers were located inside the mixing chamber in direct contact with the liquid  ${}^3\text{He}$ - ${}^4\text{He}$  mixture in order to maximize thermal contact to the sample. The mixing chamber was fabricated from nonmetallic epoxy resin (Stycast 1266, Emerson & Cuming Inc., Woburn, MA) in order to minimize Joule heating from the rf pulses. Sample access was via a resealable conical plug in the bottom of the

mixing chamber. Several NMR samples were mounted in separate coils inside the mixing chamber. They included both of the  $\text{UBe}_{13-x}\text{B}_x$  concentrations and a Pt powder NMR thermometer. Each  $\text{UBe}_{13-x}\text{B}_x$  sample consisted of  $\sim 75$  mg of loosely packed powder in a cylindrical epoxy tube; cotton wads plugged both ends allowing the  $^3\text{He}$ - $^4\text{He}$  mixture to bathe the powder grains. Copper NMR coils were wound around each sample tube and soldered to a twisted-pair transmission line that passed to the exterior of the mixing chamber. The twisted pairs were soldered to a 50- $\Omega$  CuNi coax that provided the rf connection to the laboratory.

For ease of use with the dilution refrigerator, we employed a coil impedance matching and frequency tuning system that required no variable components inside the refrigerator (“top tuning”). In the mixing chamber, the transmission line was terminated solely by the NMR coil, whose reactance was in the range 50–100  $\Omega$ , depending on frequency. At the top of the refrigerator, two adjustments were used to adjust the real part of the input impedance of the terminated line to the 50- $\Omega$  impedance of the NMR spectrometer and to cancel its imaginary part. This was accomplished by adding a variable length transmission line (“trombone”) plus a fixed length of cable, if necessary) to the connector at the top of the refrigerator and a variable capacitor at the other end of the transmission line. By adjusting these two components while measuring the input impedance with a network analyzer, the system was easily tuned and matched to 50  $\Omega$ . By using this scheme we obtained an operating quality factor ( $Q$ ) on the order of 30 and good sensitivity for the measurements.

For low-temperature thermometry we used pulsed  $^{195}\text{Pt}$  NMR as the absolute reference thermometer.<sup>13</sup> Several  $\text{RuO}_2$  (2-k $\Omega$ ) thin-film chip resistance thermometers (Dale Electronics Inc., Columbus, NE) were calibrated in temperature and magnetic field using the  $^{195}\text{Pt}$  NMR thermometer. The  $\text{RuO}_2$  thermometers were used for regulating temperature during the  $\text{UBe}_{13-x}\text{B}_x$  experiments in conjunction with a four-wire ac resistance bridge/temperature controller (LR400/LR130 Linear Research Inc., San Diego, CA) that powered a resistance heater located inside the mixing chamber.

All NMR data were acquired using two-channel (in-phase and quadrature phase) detection of the spin echo signals. For  $T_1$  measurements, the pulse sequence comb- $t$ - $\pi/2$ - $\tau$ - $\pi$ - $\tau$ -acquire-recycle was used,<sup>14</sup> where the comb consisted a series of one to fifteen  $\pi/2$  pulses. The delay time  $t$  was varied in logarithmic steps ( $\geq 12$ ) and the magnetization recovery was monitored by measuring the height of the spin echo. The recycle time was set to of order of  $5T_1$ . The spectra were obtained by taking the Fourier transform of the second half of the spin echo.

We employed several strategies to avoid and evaluate heating of the sample and/or mixing chamber by the rf pulses. Two of these strategies were to use a plastic mixing chamber to avoid eddy current heating from a metal source and to encourage good thermal contact between the grains of the sample and the liquid He mixture. On the basis of an approximate analysis,<sup>15</sup> we estimated that the time constant for thermal equilibration of the sample to the bath after a rf pulse was on the order of 0.01 s at 100 mK. Because this value is about four orders of magnitude less than typical

values of  $T_1$ , we assumed that rf heating should not degrade the  $T_1$  measurements. As a check, nevertheless, we often tested the possibility that heating might affect the measurements by adding progressively more rf pulses to the saturating train, effectively increasing the rf duty factor, until a corresponding change in the apparent value of  $T_1$  was observed. All measurements were taken with numbers of saturating pulses that were well below the number needed to exhibit rf heating effects.

Another important consideration for measurements of the Knight shift is the change in magnetic field associated with the magnetic susceptibility of the granular sample. In an applied magnetic field, the large paramagnetic susceptibility of  $\text{UBe}_{13-x}\text{B}_x$  generates a substantial demagnetization field that contributes to the local field at a powder particle. This effect dominates the  $^{11}\text{B}$  spectral linewidth at high fields<sup>6</sup> and skews the spectrum centroid position towards higher frequency.<sup>16</sup> As a way of evaluating the local field, we mixed a small amount ( $\sim 10\%$  of the volume) of high-purity (99.9%) Al powder with each powdered  $\text{UBe}_{13-x}\text{B}_x$  sample. The Al powder was used as a local field reference for the  $K_B$  measurements.

By using the  $^{27}\text{Al}$  NMR reference signal and the analysis presented below, we evaluated the correction needed to obtain accurate values of  $K_B$ . The advantage of using the  $^{27}\text{Al}$  reference is that it avoids the need to calculate the sample-geometry-dependent demagnetization field. In our measurements on loosely packed powder samples, we assumed that the average field measured by the  $^{27}\text{Al}$  powder is the same as the average field experienced by the  $\text{UBe}_{13-x}\text{B}_x$  particles. An implicit (and reasonable) assumption of this approach is that the average particle geometry is spherical and that the magnetic susceptibility of Al is negligible compared to  $\text{UBe}_{13-x}\text{B}_x$ . With these assumptions, the mean NMR frequency ( $f_{\text{Al}}$  and  $f_{\text{B}}$ ) for  $^{27}\text{Al}$  and  $^{11}\text{B}$  at constant applied field can be expressed as

$$f_{\text{Al}} = \gamma_{\text{Al}}(1 + K_{\text{Al}})(B_0 + \Delta B) \quad (1)$$

and

$$f_{\text{B}} = \gamma_{\text{B}}(1 + K_{\text{B}})(B_0 + \Delta B), \quad (2)$$

respectively, where  $\gamma_{\text{Al}}$  and  $\gamma_{\text{B}}$  are the nuclear gyromagnetic ratios,  $K_{\text{Al}}$  and  $K_{\text{B}}$  are the  $^{27}\text{Al}$  and  $^{11}\text{B}$  Knight shifts, respectively,  $B_0$  is the applied field strength, and  $\Delta B$  is the field correction due to bulk demagnetization. By combining Eqs. (1) and (2), we have

$$K_{\text{B}} = \frac{f_{\text{B}}\gamma_{\text{Al}}}{f_{\text{Al}}\gamma_{\text{B}}}(1 + K_{\text{Al}}) - 1 = \left[ 0.813\,39 \frac{f_{\text{B}}}{f_{\text{Al}}} - 1 \right], \quad (3)$$

where we have used the accepted values for  $\gamma$  and the slightly temperature-dependent values for the Knight shift of  $^{27}\text{Al}$ .<sup>16</sup> An important advantage of using this method to compensate for the bulk demagnetization field is that Eq. (3) is independent of both  $B_0$  and the sample dimensions.

### III. EXPERIMENTAL RESULTS

In this section we present results for the temperature-dependent behavior of  $T_1$  and  $K_{\text{B}}$  in the normal and superconducting states.

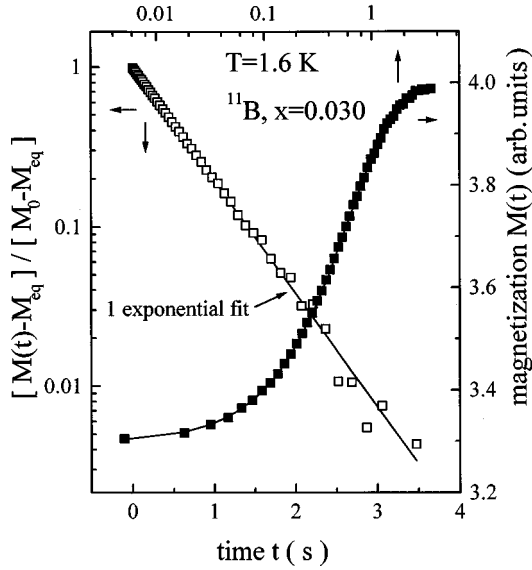


FIG. 2. Typical magnetization recovery measured by the comb-saturation-recovery method in the normal state in the  $x=0.030$  sample at 1.6 K. The recovery is accurately fit to a single exponential recovery [Eq. (4), solid line]. These data were taken at 1.47 T.

#### A. Normal state

Figure 2 shows a typical  $^{11}\text{B}$  magnetization recovery as a function of time after the magnetization has been destroyed by the comb. The recovery was fit to a single exponential of the form

$$M(t) = (M_0 - M_{\text{eq}})e^{-t/T_1} + M_{\text{eq}}, \quad (4)$$

where  $M_0$ ,  $M_{\text{eq}}$ , and  $T_1$  are the fit parameters. The accuracy in the  $T_1$  fit was typically better than  $\pm 2\%$  at all temperatures. The results of the normal state  $^{11}\text{B}$   $1/T_1$  as a function of  $T$  spanning more than three orders of magnitude in temperature are shown in Fig. 3 for the  $x=0.030$  sample. These data, along with the results for the  $x=0.067$  sample, are plotted as  $1/T_1 T$  versus  $T$  in Fig. 4.

The data below  $\sim 0.6$  K were taken in a field of 8.1 T (110.6 MHz), which exceeds  $H_{c2}$  in this temperature range ( $H_{c2} = 10.2$  T at  $T=0$ ).<sup>17</sup> The remaining data were acquired at 1.47 T between 0.7 and 1.0 K and 7 T for  $T > 1$  K. The spin-lattice relaxation rate in the normal state is field independent at least up to 9 T; this was investigated at 0.4, 1.7, and 5 K over a wide range of fields in both sample concentrations.

Several energy scales affecting the spin-lattice relaxation  $T$  dependence are evident from Fig. 3. The most striking is the rapid downturn in  $1/T_1$  occurring below  $\sim 4$  K and  $1/T_1$  appears to approach a constant value at the lowest temperatures ( $T < 0.6$  K). Also, an additional relaxation mechanism is evident above  $\sim 60$  K.

Figure 4 shows the effect of B concentration on  $1/T_1 T$ . At high temperatures there is virtually no difference between the two B concentrations; however, at temperatures of  $\sim 1$  K, there is significant sample variation. In this temperature regime,  $T_1$  for the  $x=0.030$  sample is approximately twice that of the  $x=0.067$  sample. [This same ratio  $T_1(x=0.030)/T_1(x=0.067) \sim 2$  is also seen in Fig. 7 for the  $^9\text{Be}$  at comparable temperatures.] A prominent feature of the nor-

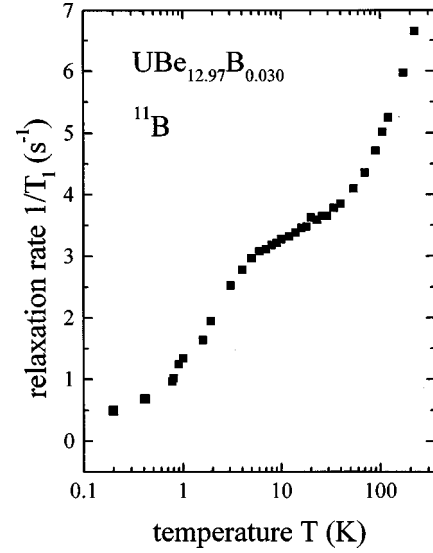


FIG. 3. Temperature dependence of  $1/T_1$  for the  $x=0.030$  sample. Several energy scales affecting the relaxation rate  $T$  dependence are evident. A rapid downturn in  $1/T_1$  occurs below  $\sim 4$  K, an additional relaxation mechanism is evident above  $\sim 60$  K, and  $1/T_1$  appears to approach a constant value at the lowest temperatures ( $T < 0.6$  K). The data below  $\sim 0.6$  K were taken at a field high enough (8.1 T) to exceed  $H_{c2}$ . The remaining data were acquired at 1.47 T between 0.7 and 1.0 K and 7 T for  $T > 1$  K.

mal state data at low  $T$  is a distinct broad maximum and monotonic decrease in  $1/T_1 T$  with decreasing  $T$ . This is one of the most surprising features of the normal state  $T_1$  results.

Above  $\sim 1$  K, the overall temperature dependence of the  $^{11}\text{B}$   $T_1$  looks qualitatively similar to what is observed for  $^9\text{Be}$  in undoped  $\text{UBe}_{13}$ .<sup>11,12</sup> The undoped material shows a nar-

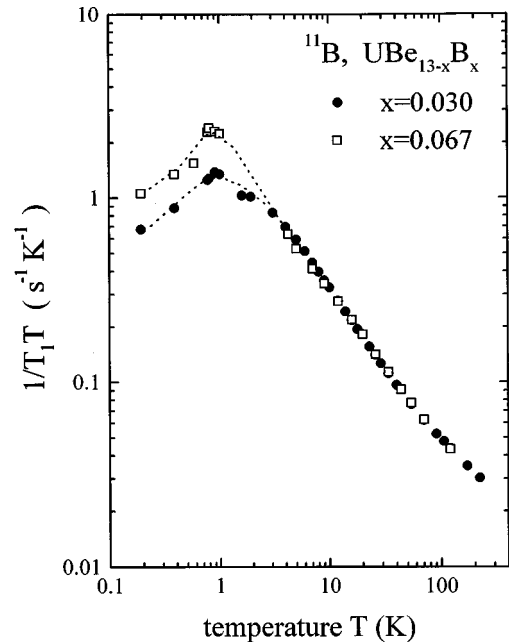


FIG. 4. Temperature dependence of  $1/T_1 T$  for  $x=0.030$  (solid circles) and 0.067 (open squares). At low temperatures  $1/T_1 T$  differs by  $\sim 2$  between the two samples, but shows no difference at higher temperatures.  $1/T_1 T$  goes through a broad maximum centered at approximately 1 K.

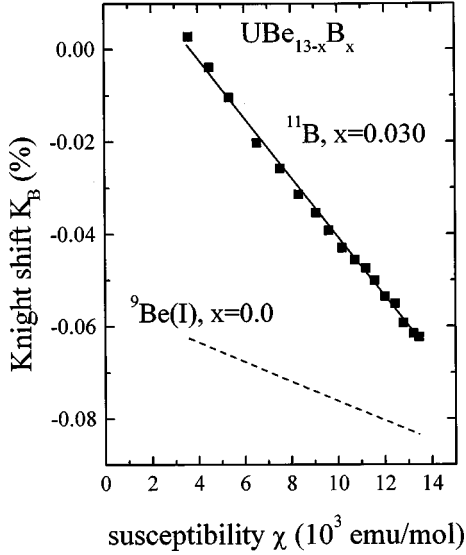


FIG. 5.  $K_B$  versus  $\chi$  for the  $x=0.030$  sample. The slope gives the hyperfine coupling constant, which is equal to  $-361.1 \text{ Oe}/\mu_B$ . The data for the undoped material are taken from Ref. 10 and were measured in a single crystal. The  $x=0.067$  sample (not shown) exhibits quantitatively similar behavior.  $K_B$  was calculated using Eq. (3) with an uncertainty estimated at  $\pm 0.008\%$ . The Knight shift data in Fig. 5 are isotropic shifts. The linearity of  $K_B$  versus  $\chi$  implies that a single mechanism is responsible for the  $T$  dependence of both  $K_B$  and  $\chi$ . The data were acquired at  $B_0=7 \text{ T}$ .

row temperature range spanning less than 2 K just above  $T_c$  where  $1/T_1 T$  is roughly constant.<sup>8</sup> At higher temperatures,  $1/T_1$  is nearly independent of temperature up to approximately  $\sim 60 \text{ K}$ ; above this temperature,  $1/T_1$  is more strongly temperature dependent. The additional relaxation occurring above  $\sim 60 \text{ K}$  has been attributed to thermal excitations of low-lying crystal field states of the  $\text{U}^{3+}$  ion.<sup>11</sup> The downturn in  $1/T_1 T$  below  $\sim 2 \text{ K}$  that we observe has not been previously reported to our knowledge.

Figure 5 shows  $K_B$  plotted as a function of  $\chi(T)$  in the  $x=0.030$  sample with temperature the implicit parameter over the range 4.2–300 K. The  $x=0.067$  sample (not shown) has a comparable magnitude of shift and temperature dependence.  $K_B$  was calculated using Eq. (3) with an uncertainty estimated at  $\pm 0.008\%$ . For comparison, the dashed line in Fig. 5 shows the  $^9\text{Be}$  data for the Be(I) site in undoped single-crystal  $\text{UBe}_{13}$ .<sup>10</sup> Because the Be(I) site has local cubic symmetry, the Knight shift data in Fig. 5 for both nuclei are isotropic shifts. The linearity of the  $K_B$  versus  $\chi$  plot suggests that a single mechanism is responsible for the  $T$  dependence of both the Knight shift and the magnetic susceptibility.

From the slope of the  $K_B$  versus  $\chi$  plot, we calculate the value of the hyperfine coupling constant. The susceptibility can be decomposed into a summation of temperature independent and dependent terms

$$\chi(T) = \chi_0 + \chi_{sf}(T), \quad (5)$$

where  $\chi_0$  has contributions from  $T$ -independent diamagnetic and orbital susceptibility. The term  $\chi_{sf}(T)$  has contributions from conduction electron and  $f$ -electron (Curie-Weiss) paramagnetism. In heavy fermions, strong hybridization between

conduction and  $f$  electrons at low temperatures makes it reasonable to combine these two contributions into a single  $T$ -dependent term. The Knight shift, which is proportional to the magnetic susceptibility, can be expressed as

$$K_B(T) = K_0 + K_{sf}(T) = K_0 + \frac{H_{\text{hf}} \chi_{sf}(T)}{N \mu_B}, \quad (6)$$

where  $H_{\text{hf}}$  is the hyperfine field,  $N$  is Avogadro's number, and  $\mu_B$  is the Bohr magneton. Using Eq. (6) and the slope of the  $^{11}\text{B}$  data in Fig. 5, we obtain  $H_{\text{hf}} = -361.1 \text{ Oe}/\mu_B$ .

## B. Superconducting state

In this section we present measurements of  $1/T_1$  and the Knight shift in the superconducting state to provide insight into how a small concentration of B modifies the superconducting density of states. We focus on the  $1/T_1$  data from the  $^9\text{Be}$  and  $^{11}\text{B}$  nuclei in  $\text{UBe}_{13-x}\text{B}_x$  for  $x=0.030$  and  $0.067$  in the temperature range between 0.096 and 2 K. Also,  $^{11}\text{B}$  Knight shift data for the two samples are presented in the same temperature regime.

Note that for the following data  $^{11}\text{B}$  measures properties at the Be(I) site, whereas  $^9\text{Be}$  primarily measures the more abundant Be(II) sites. Selective excitation of one site or the other is not easily achieved for the  $^9\text{Be}$ , so that one-thirteenth of the total nuclear magnetization originates from Be(I).

For the  $T_1$  measurements, all Zeeman levels were saturated and the magnetization recovery was recorded as a function of time. Unlike the  $T_1$  measurements in the normal state, the recovery in the superconducting state exhibited a distribution of relaxation times for both samples and nuclei that were investigated. A reasonable fit to the actual recovery is obtained using the double exponential expression

$$M(t) = M_{\text{eq}}^{(l)}(1 - e^{-t/T_1^{(l)}}) + M_{\text{eq}}^{(s)}(1 - e^{-t/T_1^{(s)}}) + M_0, \quad (7)$$

where  $M_{\text{eq}}^{(l)}$ ,  $M_{\text{eq}}^{(s)}$ ,  $M_0$ ,  $T_1^{(l)}$ , and  $T_1^{(s)}$  are fit parameters. Here  $s$  denotes the short time constant and  $l$  is the long one.

A typical example of such a recovery that covers over five orders of magnitude in time is shown in Fig. 6, where the echo signal height is plotted as a function of  $t$  at 0.192 K with  $B_0=1.47 \text{ T}$ . The solid line, which shows the double exponential fit, works well for the later times, but has a visible deviation at shorter times that reflects a distribution of short relaxation times. This situation is reflected in the uncertainties in the fit. At this temperature, the uncertainty is  $\pm 10\%$  for  $T_1^{(s)}$  and  $\pm 1.6\%$  for  $T_1^{(l)}$ . Also, the values of  $T_1^{(s)}$  and  $T_1^{(l)}$  differ by at least an order of magnitude throughout most of the temperature range below  $T_c$ . The relative weight of  $M_{\text{eq}}^{(l)}/M_{\text{eq}}^{(s)}$  is of order unity at this temperature, but more generally varies in the range 0.1–2 depending upon the nucleus, the value of  $x$ , and  $T$ .<sup>18</sup> These features of the magnetization recovery were observed for both  $^{11}\text{B}$  and  $^9\text{Be}$  in the two samples studied, as well as in our own measurements of undoped  $\text{UBe}_{13}$ . In undoped  $\text{UBe}_{13}$ , the long time constant agreed with previously reported results.<sup>8</sup>

We employed two tests that showed that the origin of the  $T_1$  distribution is not transient Joule heating by the rf pulses. First, we intentionally induced sample heating by the rf pulses during a  $T_1$  measurement and investigated its signa-

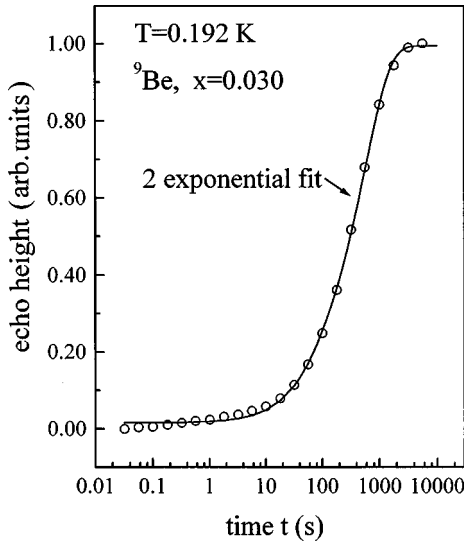


FIG. 6. Typical magnetization recovery measured by the comb-saturation-recovery method in the superconducting state in the  $x = 0.030$  sample at 0.192 K. The recovery exhibits a distributed  $T_1$  behavior. Two exponentials [Eq. (7)] were used to fit superconducting data. We assume that the longer time constant is representative of the quasiparticle relaxation and the  $T$  dependence of this quantity is displayed in subsequent figures. These data were taken at 1.47 T.

ture on the parameters in Eq. (7). Sets of  $T_1$  data were recorded as a function of rf power by varying the number of pulses ( $N_p$ ) in the saturating train. The fitting parameters were essentially constant for  $N_p = 5-20$ . When  $N_p = 40$ , there was evidence of transient heating by the rf pulses. (Also, a small transient increase in the temperature of the mixing chamber's thermometer was observed immediately following the train of 40 pulses.) There was also an anomaly for  $N_p = 1$  that we interpret as spectral diffusion following incomplete saturation of the inhomogeneously broadened  $^9\text{Be}$  spectrum ('hole burning').

The second indication that the distribution in  $T_1$  is not related to heating is that at constant temperature, increasing the magnetic field above  $H_{c2}$  returns the recovery to single exponential. Joule heating, which is proportional to the square of the frequency, should become worse at the higher frequency needed to exceed  $H_{c2}$ . Thus we attribute the distributed  $T_1$  as relating to the superconducting state.

Here we concentrate on the properties of the long time constant (referred to simply as  $T_1$ ), whose primary origin we attribute to spin-lattice relaxation by thermally excited quasiparticles outside of the vortex core region of the superconductor. The typical uncertainty in the individual measurements is on the order of 2%.

Figures 7 and 8 show the temperature dependence of  $1/T_1$  at 1.47 T for  $^9\text{Be}$  and  $^{11}\text{B}$ , where  $T_1 = T_1^{(l)}$ . Values of  $N_p$  were chosen to avoid rf heating and incomplete saturation of the NMR line. Below  $T_c$  there is a sharp decrease in  $1/T_1$  for both  $^9\text{Be}$  and  $^{11}\text{B}$ . This abrupt drop just below  $T_c$  is most likely an artifact caused by the change from the single exponential behavior above  $T_c$  to multiple exponential just below it. The use of a double exponential analysis close to the transition is problematic because the separation of the slow and fast parts is less evident than it is at lower temperatures. Therefore, the sharpness of the initial drop in the range

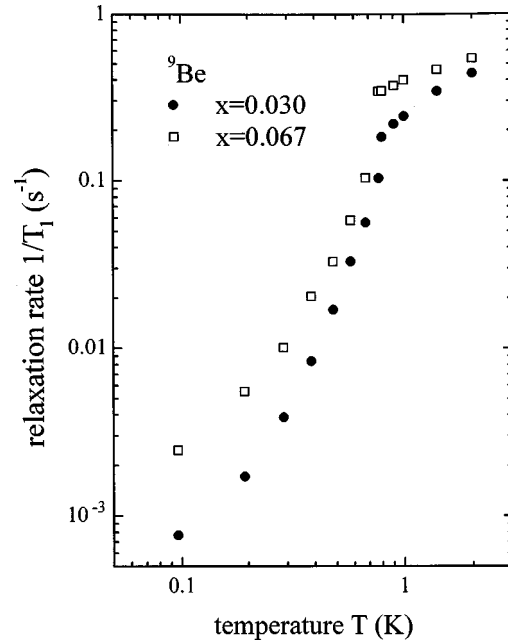


FIG. 7. Temperature dependence of  $1/T_1$  for  $^9\text{Be}$ . Note that there is not a significant span of temperature where a power-law  $T$  dependence is obeyed. Also, there is a significant difference in the magnitude and the temperature dependence of  $1/T_1$  between the two B concentrations; in the normal state at  $T \sim 1$  K,  $T_1(x = 0.030)/T_1(x = 0.067) \sim 2$ . The abrupt drop immediately below  $T_c$  is most likely an artifact, as discussed in Sec. III B. The data were acquired at  $B_0 = 1.47$  T.

$0.9T_c - 1.0T_c$  should be discounted. At lower temperatures, however, where the analysis provides an unambiguous value for  $1/T_1$ , there is no significant span of temperature where  $1/T_1 \propto T^3$ , as reported for undoped  $\text{UBe}_{13}$ .<sup>8</sup>

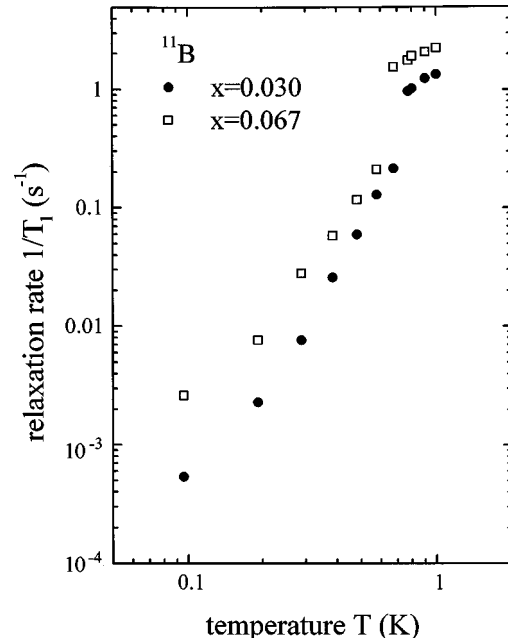


FIG. 8. Temperature dependence of  $1/T_1$  for  $^{11}\text{B}$ . The overall behavior of the two concentrations looks very similar to the  $^9\text{Be}$  data (see the caption of Fig. 7). The data were acquired at  $B_0 = 1.47$  T.

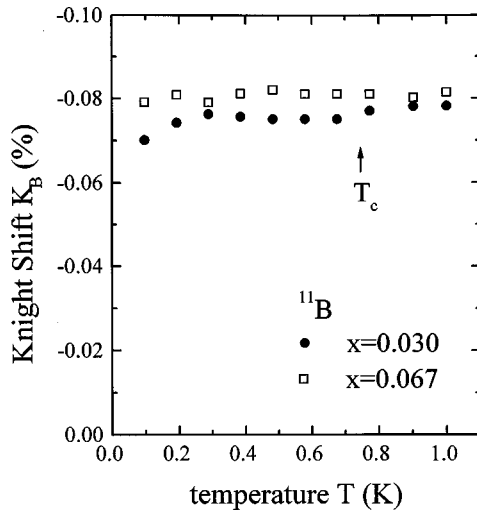


FIG. 9. Temperature dependence of  $K_B$  in the superconducting state. The  $K_B$  was measured with respect to the  $^{27}\text{Al}$  resonance and calculated using Eq. (3). The data show no significant temperature variation in the superconducting state. Both B concentrations have the same shift within the uncertainty, which is estimated to be  $\pm 0.01\%$ . The data were taken at 1.47 T.

The  $^{11}\text{B}$  magnetic shift measurements in the superconducting state were made for both sample concentrations and in the same temperature range as the  $1/T_1$  data. The results are displayed in Fig. 9. The superconducting diamagnetic shift was accounted for using an Al powder reference [Eq. (3)]. However, the magnitude of the superconducting diamagnetic shift was negligible because no detectable shift in the  $^{27}\text{Al}$  resonance position was observed upon entering the superconducting state. This behavior is a consequence of the large Ginzburg-Landau parameter ( $\kappa \sim 100$ ) for this material.<sup>19</sup> Figure 9 shows a temperature-independent shift in the superconducting state equal to the normal state value near  $T_c$ . The magnitude of the shift is  $-0.08$  ( $\pm 0.01\%$ ) and is comparable for both samples. For the  $x=0.067$  sample there is a tendency for a slightly more negative shift, but this is probably not significant and is within the stated uncertainty. The spectral linewidths and line shapes also remain constant below  $T_c$ . The linewidths in an applied field of 1.47 T are  $10.7 \pm 0.7$  and  $11.7 \pm 1.2$  G for the  $x=0.030$  and 0.067 samples, respectively. A small amount of broadening is expected at low temperatures due to the magnetic field distribution of the vortex lattice. However, this effect would be small due to the large penetration depth of these materials<sup>20</sup> and is not resolvable in our measurements.

#### IV. ANALYSIS AND DISCUSSION

In this section we analyze and interpret the normal and superconducting state properties investigated by our NMR measurements.

##### A. Normal state

The values of  $1/T_1$  for the  $^9\text{Be}$  in the  $x=0.030$  sample (Fig. 7) are almost the same as those in the normal state of undoped  $\text{UBe}_{13}$  (Ref. 8) at all temperatures investigated. In contrast, just above  $T_c$  the  $x=0.067$  sample (Fig. 7) has a

value for  $1/T_1$  of  $^9\text{Be}$  that is roughly twice that of the  $x=0.030$  sample or the undoped material; a factor of 2 increase is also observed in the  $^{11}\text{B}$   $T_1$  results (Figs. 4 and 8). Interestingly, the  $^9\text{Be}$   $T_1$  for  $x=0.067$  is similar to what is observed in  $\text{U}_{0.967}\text{Th}_{0.033}\text{Be}_{13}$ .<sup>8</sup>

Above  $\sim 4$  K, the  $T_1$  values for either  $^9\text{Be}$  or  $^{11}\text{B}$  for both B concentrations are indistinguishable within experimental uncertainties. The apparent upturn in  $1/T_1$  observed at  $\sim 60$  K (Fig. 3) occurs essentially at the same  $T$  as undoped  $\text{UBe}_{13}$  (Ref. 11) and suggests that there is not a significant modification of the crystal field level splitting with B doping. We note that a similar conclusion was reached after inspection of the high-temperature resistivity data in the same samples.<sup>5</sup> Thus, only at temperatures below  $\sim 4$  K do measurements of  $1/T_1$  show significant differences between the two samples.

The maximum in  $1/T_1 T$  (Fig. 4) observed in both samples is not understood. Because  $T_1$  probes the density of states (DOS) close to the Fermi energy ( $\epsilon_F$ ), this behavior is consistent with “structure” in the many-body resonance at  $\epsilon_F$  and/or a slight displacement of the resonance away from  $\epsilon_F$ . In the latter case, the displacement would be of order of a few tenths of a degree kelvin away from  $\epsilon_F$ . Also, this behavior could be explained by a slight temperature dependence to the amplitude or position of the resonance at low temperatures.

The spin-lattice relaxation rate in the normal state is independent of magnetic field up to the limit of 9 T covered in our experiments. This behavior has been investigated at 0.4, 1.7, and 5 K, over a wide range of fields and in both samples. Similar results have been observed in the undoped material.<sup>21</sup> This result is consistent with nonsaturation of the magnetization with increasing field strength. The NMR shows that a narrow, rigid, spin-split band does *not* describe the states near the Fermi energy that are responsible for the heavy-fermion properties. An explanation of this behavior is certainly one of the most interesting outstanding questions concerning the normal state of  $\text{UBe}_{13}$ .

The normal state  $K_B$  and hyperfine field data (Fig. 5) show several interesting features. First, the magnitude of the hyperfine field calculated for  $^{11}\text{B}$  ( $-361.1 \text{ Oe}/\mu_B$ ) is approximately a factor of 3 larger than that of the Be(I) site in undoped  $\text{UBe}_{13}$  ( $-118 \text{ Oe}/\mu_B$ ).<sup>10</sup> This result cannot be explained in terms of differences in the magnitude of the atomic hyperfine fields for the two different atoms, which should be comparable because they have the same core electron configuration. (Be and B are neighbors on the Periodic Table.) Because  $K_B \propto \chi \langle |\psi_s(0)|^2 \rangle$  (the bracketed term is the square of the electronic wave function at the nucleus averaged over the Fermi surface) and the bulk susceptibility of these samples are the same, the value of  $\langle |\psi_s(0)|^2 \rangle$  must be larger for  $^{11}\text{B}$  than for  $^9\text{Be}$ . The reason for this is not clear, but perhaps the extra  $2p$  electron from the B adds an additional core-polarization contribution to the hyperfine field. Another possibility is that because of the larger valence of B compared to Be, the B impurity requires extra electron density locally to screen the excess charge; this could possibly increase the size of the contact hyperfine term.

It is also noteworthy that the sign of the shifts and hyperfine fields is negative for both the  $^{11}\text{B}$  and the undoped Be(I) site. Interestingly, for the Be(II) site in pure  $\text{UBe}_{13}$ , the shifts

and hyperfine fields are all positive.<sup>10</sup> The negative sign at the Be(I) site for both nuclei indicates an opposite sign for the electronic spin density with respect to the applied field at that specific lattice position.

### B. Uranium moment fluctuation rate

By combining the results of the  $T_1$ ,  $K_B$ , and  $\chi$  measurements, we estimate the U moment fluctuation rate using the following analysis. The dominant mechanisms responsible for  $T_1$  in UBe<sub>13-x</sub>B<sub>x</sub> are assumed to be composed of primarily two terms

$$\frac{1}{T_1} = \left( \frac{1}{T_1} \right)_{\text{on-site}} + \left( \frac{1}{T_1} \right)_{\text{dip}}. \quad (8)$$

The first contribution, or ‘‘on-site’’ term, involves a fluctuating electron spin density directly overlapping the nuclei. This term can have several origins including fluctuations of the conduction electrons arising from the exchange interaction with the  $5f$  electrons. The second term is the direct nuclear coupling to the fluctuating moment via the dipolar interaction.

The on-site term can be obtained from<sup>22</sup>

$$\frac{1}{T_1} = \frac{k_B \gamma_n^2 T}{\mu_B^2} \sum_q |H_{\text{hf}}(q)|^2 \lim_{\omega_n \rightarrow 0} \left[ \frac{\chi''(q, \omega_n)}{\omega_n} \right], \quad (9)$$

where  $k_B$  is Boltzmann’s constant,  $\gamma_n$  is the nuclear gyromagnetic ratio,  $\mu_B$  is the Bohr magneton,  $\chi(q, \omega) = \chi'(q, \omega) + i\chi''(q, \omega)$  is the dynamic susceptibility,  $H_{\text{hf}}(q)$  is the Fourier transform of the spatially dependent hyperfine field, and  $\omega_n$  is the Larmor frequency. We assume that the fluctuations of neighboring U moments are uncorrelated, which implies that  $\chi$  is independent of  $q$ . The electronic fluctuation time can be expressed as

$$\tau = \lim_{\omega_n \rightarrow 0} \left[ \frac{\chi''(\omega_n)}{\chi'(0)\omega_n} \right], \quad (10)$$

where  $\chi'(0)$  is the static susceptibility per U atom. The dipolar term can be obtained using the expression<sup>23</sup>

$$\left( \frac{1}{T_1} \right)_{\text{dip}} = 4\gamma_n^2 k_B T \left( \sum_i \frac{1}{r_i^6} \right) \lim_{\omega_n \rightarrow 0} \left[ \frac{\chi''(\omega_n)}{\omega_n} \right], \quad (11)$$

where  $r_i$  is the magnitude of the position vector joining the nucleus and the  $i$ th fluctuating electronic spin.

By combining Eqs. (8)–(11), an approximate relation for the fluctuation rate  $\Gamma \equiv \hbar/\tau$  can be derived,

$$\Gamma \approx 2\gamma_n^2 k_B \hbar \left[ \frac{2N}{r_N^6} + \frac{H_{\text{hf}}^2}{\mu_B^2} \right] T_1 T \chi'(0), \quad (12)$$

where  $N$  is the number of nearest-neighbor U atoms at a distance  $r_N$ , and  $H_{\text{hf}}$  is the isotropic hyperfine field obtained from the Knight shift. A number of assumptions are contained within Eq. (12); the most important are (i) a  $q$ -independent  $\chi$  (discussed further below), (ii) both relaxation mechanisms in Eq. (8) can be described in terms of a single fluctuation time ( $\tau$ ), (iii) only nearest-neighbor contributions are included in the dipolar term, and (iv) the elec-

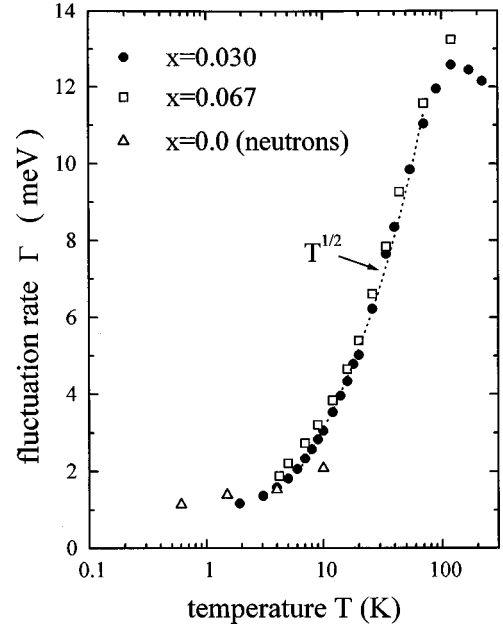


FIG. 10. Temperature dependence of the electronic fluctuation rate for the  $x=0.030$  (solid circles) and  $0.067$  (open squares) samples. The  $\sqrt{T}$  dependence at intermediate temperatures is characteristic of local moment fluctuations. At low temperatures,  $\Gamma$  is consistent with the value of the renormalized density of states obtained by thermodynamic measurements. Above  $\sim 60$  K, the effects of crystal fields are observed. Also shown is the quasielastic line-width data from neutron scattering results in UBe<sub>13</sub> (open triangles) (Ref. 26), which are in reasonable agreement with values obtained by NMR.

tronic spin is a point moment. We estimate that the error associated with these assumptions is much less than an order of magnitude.

Figure 10 show the values of  $\Gamma$  obtained from Eq. (12) and using the experimental results in Figs. 3–5. A strong temperature dependence of  $\Gamma$  is observed. Roughly between 8 and 70 K  $\Gamma \propto \sqrt{T}$ . A similar temperature dependence is also seen in many Ce-, Yb-, and U-based heavy-fermion compounds<sup>12,24</sup> at temperatures greater than the coherence temperature. This temperature dependence can be deduced theoretically using a single-impurity degenerate Anderson model<sup>25</sup> and is universal for a temperature regime larger than the system’s Kondo temperature. The observation of a  $\sqrt{T}$  dependence in UBe<sub>13-x</sub>B<sub>x</sub> suggests the existence of isolated local moment fluctuations at high temperatures. At temperatures above 70 K the presence of crystal field splittings introduces an additional energy scale that destroys the  $\sqrt{T}$  dependence. At low temperatures,  $\Gamma$  approaches a constant value of order of 1 meV or 10 K, which is consistent with the order of magnitude of the renormalized density of states obtained by thermodynamic measurements.

It is interesting to estimate the relative contributions to  $1/T_1$  from the on-site and dipolar terms of Eq. (8). By using the above assumptions, we obtain for this ratio

$$\frac{\left( \frac{1}{T_1} \right)_{\text{on-site}}}{\left( \frac{1}{T_1} \right)_{\text{dip}}} = \frac{1}{2} \frac{H_{\text{hf}}^2 r_N^6}{N \mu_B^2} \sim 0.7, \quad (13)$$

where  $H_{\text{hf}} = -361.1$  Oe,  $N = 8$ , and  $r_N = 4.4$  Å, which is the Be(I)-U separation. Thus both the on-site and dipolar terms have a comparable contribution to the total relaxation rate.

Measurements of  $1/T_1$  indicate a moderate decrease in  $\Gamma$  upon doping with boron. At low temperatures in the normal state,  $1/T_1$  of  $^9\text{Be}$  is about the same for the undoped material and for  $x=0.030$ . On the other hand, the  $x=0.067$  sample has a value of  $1/T_1$  about twice that of the  $x=0.030$  sample for both  $^9\text{Be}$  and  $^{11}\text{B}$ . However, as is the case for the static magnetic susceptibility,<sup>5</sup> there is no change in  $K_B$  with B concentration. Thus we estimate that  $\Gamma$  for the  $x=0.030$  sample is roughly equal to that of undoped  $\text{UBe}_{13}$  and  $\Gamma(x=0.030)/\Gamma(x=0.067) \sim 2$ .

Under certain conditions  $\Gamma$  calculated from NMR parameters can be compared to the results of neutron scattering quasielastic linewidth measurements. NMR and neutrons probe somewhat different aspects of the imaginary part of the dynamic susceptibility  $\chi''(q, \omega)$ . Quantitative agreement between the two probes is observed if  $\chi''$  is independent of  $q$  and the fluctuation spectrum, given by Eq. (10), is Lorentzian in form. For neutrons, the half-width at half maximum of the quasielastic response, which is a measure of the fluctuation rate of the system, is the relevant quantity to be compared to the NMR results.

Neutron scattering experiments have not been performed in  $\text{UBe}_{13-x}\text{B}_x$ . However, low-energy quasielastic linewidth measurements have been made in undoped  $\text{UBe}_{13}$ .<sup>26</sup> In Fig. 10 the results of these measurements, averaged over the different  $q$  values at each temperature, are compared to the  $\Gamma$  values estimated from the NMR parameters for the  $x=0.030$  sample. The comparison shows reasonable agreement between the two probes, which suggests that any antiferromagnetic correlations in these materials are, at most, weak down to at least  $\sim 2$  K. This interpretation is also supported by the neutron results, which show no statistically significant variation of  $\Gamma$  with  $q$ .<sup>26</sup> Such a result is somewhat surprising since strong antiferromagnetic correlations are observed in many other heavy-fermion systems.<sup>27</sup>

In addition to the low-energy excitations observed by neutrons, a higher-energy broad magnetic response,  $\sim 13$  meV, is reported by Goldman *et al.*<sup>28</sup> in  $\text{UBe}_{13}$ . This is thought to originate from inelastic scattering from the  $\Gamma_6 \leftrightarrow \Gamma_8$  crystal field levels.<sup>26</sup> Thermal occupation of these states is evident in the  $1/T_1$  (Fig. 3) above  $\sim 60$  K, as well as in the  $\Gamma$  calculated from the NMR parameters at temperatures above  $\sim 70$  K. Thus both the low- and high-energy magnetic responses observed in neutron scattering can be detected using NMR.

### C. Superconducting state

The major result in the superconducting state is the substantial increase in  $1/T_1$  at low temperatures caused by the dilute substitution of B for Be(I) atoms. This increase may be caused by a change in the quasiparticle spectrum or by other mechanisms, such as spin diffusion to paramagnetic centers or spin diffusion to mixed-state vortex cores.<sup>29</sup>

There are several circumstances that limit the importance of relaxation by either of the two spin-diffusion mechanisms. In the case of spin diffusion to paramagnetic centers, at the 1.47-T field used in these measurements, the Zeeman splitting of a  $g=2$  magnetic moment is  $\sim 2$  K; this is much larger

than  $k_B T$  for the low-temperature regime under consideration. Under these circumstances, the paramagnetic centers are aligned with the field and the fluctuations needed for a significant contribution to  $1/T_1$  are frozen out, as seen in the case of Gd-doped  $\text{UBe}_{13}$ .<sup>30</sup> Although relaxation via spin diffusion to vortex cores can be a significant process for the  $^9\text{Be}$  spins at the lowest temperatures investigated,<sup>31</sup> it is expected to be negligible for the  $^{11}\text{B}$  nuclei. This is because the dilute concentration of the B results in a greatly reduced nuclear spin diffusion coefficient in comparison to the  $^9\text{Be}$  spins. Thus we attribute the observed increase in  $1/T_1$  at low temperatures to an increased DOS at the Fermi energy caused by the replacement of Be(I) atoms by B.

Before analyzing our results on the basis of this hypothesis, we point out several important considerations. In conventional  $s$ -wave superconductors, nonmagnetic impurities have a weak effect on fundamental parameters such as the energy gap and  $T_c$ .<sup>32</sup> Paramagnetic impurities, on the other hand, are Cooper pair breakers and result in a strong depression of  $T_c$  and a broadening of the superconducting DOS.<sup>33</sup> The situation is quite different for anisotropic superconductors. Nonmagnetic impurities can act as pair breakers and modify the low-temperature superconducting properties, even for very small impurity concentrations.<sup>34</sup> It has been argued that certain impurities in heavy-fermion systems are likely to be strong resonant scatterers with phase shifts close to  $\pi/2$ .<sup>35</sup> For such a situation, an infinitesimally small impurity concentration can result in a peak in the DOS at zero energy.<sup>34</sup> The height of this peak is proportional to the impurity concentration. At higher energies, the DOS is almost unaffected by the impurities. In terms of the NMR properties, the usual power-law dependences to  $1/T_1$  just below  $T_c$  are expected, followed by a crossover to  $1/T_1 T \sim \text{const}$  at low temperatures. Also, the Knight shift should not go to zero at  $T=0$  (assuming spin-singlet pairing) because the low-energy DOS contributes a finite spin susceptibility. Such behavior in  $1/T_1$  and the Knight shift has been observed in several cuprate superconductors.<sup>36</sup>

Figures 11 and 12 again show the low-temperature relaxation data for  $^9\text{Be}$  and  $^{11}\text{B}$ . Here we plot  $R_s/R_n \equiv (1/T_1 T)_s / (1/T_1 T)_n$  as a function of temperature, where the subscripts  $n$  and  $s$  refer to the normal state value at  $T_c$  and the superconducting state, respectively. Note that for either nuclei below  $\sim 0.2$  K,  $R_s/R_n$  approaches nearly a constant value that is strongly  $x$  dependent. At the lowest temperature of 0.096 K, the ratio

$$\rho \equiv \frac{\left(\frac{R_s}{R_n}\right)_{x=0.030}}{\left(\frac{R_s}{R_n}\right)_{x=0.067}} \quad (14)$$

is equal to 0.57 for  $^9\text{Be}$  and 0.40 for  $^{11}\text{B}$ . The low-temperature behavior seen for  $^9\text{Be}$  and  $^{11}\text{B}$ , or  $R_s/R_n$  approaching a constant, suggests a finite DOS at zero energy, or a gapless superconducting state. The number of states at low energy appear to be strongly dependent on the concentration of B impurities. Let us now focus on this low-temperature behavior and the effect of adding impurities into anisotropic superconductors.

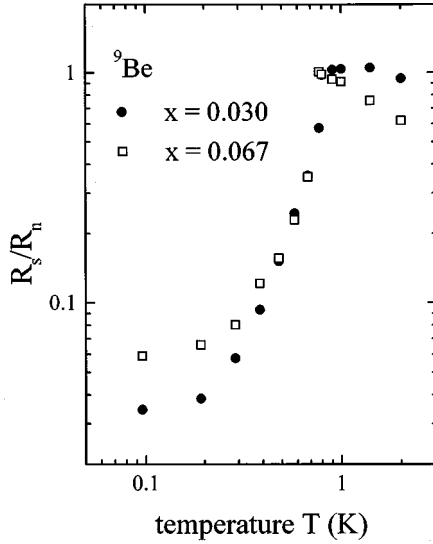


FIG. 11. Temperature dependence of  $R_s/R_n = (1/T_1 T_s)/(1/T_1 T_n)$  for  ${}^9\text{Be}$ . The subscript  $s$  represents superconducting state and  $n$  is the normal state value just above  $T_c$ . Note that below  $T_c$  the normalized relaxation rates of the two concentrations have a similar temperature dependence and magnitude, but at lower temperatures there is a substantial difference between the two rates.

Our observed low-temperature behavior of  $T_1$  is consistent with the hypothesis that the B impurities act as strong scattering centers. Assuming this to be the case, we estimate the magnitude of  $\rho$ , defined by Eq. (14), from the known B concentrations using the results of a model for resonant impurities in  $d$ -wave superconductors.<sup>37</sup> At low temperatures<sup>37</sup>

$$\frac{R_s}{R_n} \sim \left[ \frac{N_{\text{imp}}(0)}{N_0} \right]^2 \quad (15)$$

and

$$\frac{N_{\text{imp}}(0)}{N_0} \sim \sqrt{n_i}, \quad (16)$$

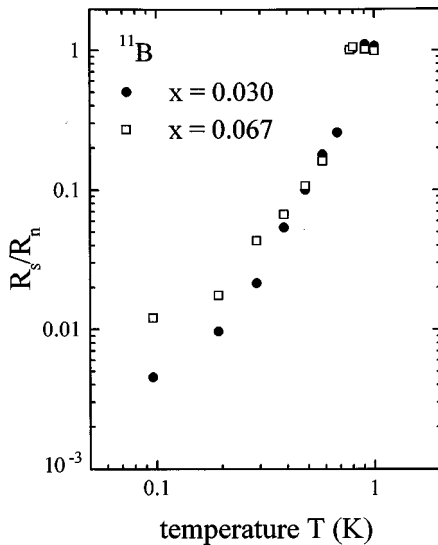


FIG. 12. Temperature dependence of  $R_s/R_n$  for  ${}^{11}\text{B}$  (see the caption of Fig. 11).

where  $N_0$  is the normal state DOS at the Fermi surface,  $N_{\text{imp}}(0)$  is the DOS at zero energy in the superconducting state, and  $n_i$  is the concentration of impurities. Therefore, we expect

$$\rho \sim \frac{(n_i)_{x=0.030}}{(n_i)_{x=0.067}}, \quad (17)$$

or just the ratio of the B concentrations, which is equal to 0.42. This value is in reasonable agreement with  $\rho=0.40$  obtained from the  ${}^{11}\text{B}$  data. For  ${}^9\text{Be}$ ,  $\rho=0.57$ , which is in poorer agreement, but we expect  ${}^9\text{Be}$  to be more affected by the other relaxation mechanisms discussed at the beginning of this section. Thus there is semiquantitative agreement of our low-temperature  $1/T_1$  data with a model calculation for resonant scattering in anisotropic superconductors.

There are several comments to be made regarding the possibility of resonant impurity scattering in  $\text{UBe}_{13-x}\text{B}_x$ . First, the impurities should be pair breakers that cause a reduction of  $T_c$ . Doping  $\text{UBe}_{13}$  with B is unusual, however, because a substantial reduction in  $T_c$  does *not* occur, which is in contrast to what happens when other nonmagnetic substitutions are made onto a U or Be site at comparable concentrations. On the other hand, Hirschfeld *et al.*<sup>34</sup> have pointed out that  $T_c$  may only be slightly depressed if impurity concentrations are at the  $10^{-3} - 10^{-4}$  level. This range is close to that of our samples. Second, if a ‘‘Kondo hole’’ picture<sup>35</sup> is relevant in this system, a B impurity must somehow behave as if it were a Kondo hole, even though the atom that it replaced does not have a moment. We speculate that the presence of the B dopant somehow substantially modifies or destroys one or more nearby U moments.

Resonant impurity scattering in  $\text{UBe}_{13-x}\text{B}_x$  should manifest itself in other measurable properties, such as very-low-temperature specific heat and thermal conductivity. In the case of specific heat, a residual linear term is expected at low temperatures. Although we are not aware of such measurements in  $\text{UBe}_{13-x}\text{B}_x$ , low-temperature ( $T \sim 90$  mK) measurements in  $\text{U}_{1-x}\text{Th}_x\text{Be}_{13}$  (Ref. 38) have shown a large linear term in  $C(T)$  for  $x > 0.02$  along with deviations in the  $T^3$  dependence normally observed in undoped  $\text{UBe}_{13}$ . Thus, in the Th-doped system, there are several suggestive characteristics of the resonant impurity scattering interpretation.

The ratio of relaxation times for  ${}^{11}\text{B}$  and  ${}^9\text{Be}$  for both B concentrations is shown in Fig. 13. For temperatures above and just below  $T_c$  the observed ratio is  $\sim 0.2$ . For magnetic relaxation, one expects this relaxation time ratio to be temperature independent and have a magnitude of order

$$\frac{T_1({}^{11}\text{B})}{T_1({}^9\text{Be})} \sim \frac{(\gamma_n H_{\text{hf}})^2|_{\text{Be}}}{(\gamma_n H_{\text{hf}})^2|_{\text{B}}} \sim 0.3, \quad (18)$$

where we have used  $H_{\text{hf}} = 478 \text{ Oe}/\mu_B$  for  ${}^9\text{Be}$  at the Be(II) site.<sup>10</sup> This is not far from the measured result in this temperature range. The large increase in this ratio at low temperatures indicates that the  ${}^9\text{Be}$  experiences ‘‘additional’’ relaxation. We attribute this to spin diffusion to vortex cores that does not affect the  ${}^{11}\text{B}$  rate because of its very small spin diffusion coefficient, as discussed above. For this reason, we believe that the  ${}^{11}\text{B}$   $T_1$  data are a more accurate measure of the intrinsic quasiparticle relaxation than the  ${}^9\text{Be}$  data.

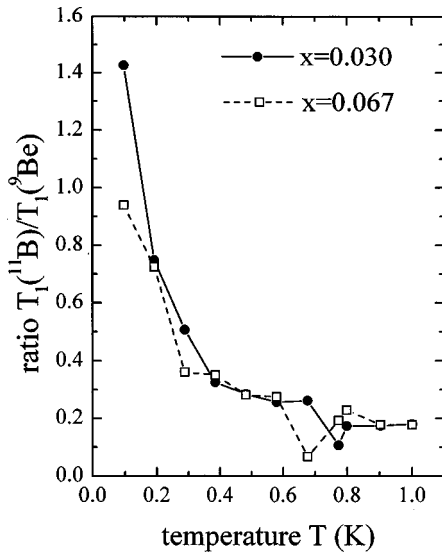


FIG. 13. Temperature dependence of the ratio of  $T_1$ 's for the  $^{11}\text{B}$  and  $^9\text{Be}$ . At low temperatures the  $^9\text{Be}$  experiences additional relaxation compared to  $^{11}\text{B}$ . We attribute this to spin diffusion to vortex cores that does not affect the  $^{11}\text{B}$  rate because of its very dilute concentration.

The main feature of  $K_B$  in  $\text{UBe}_{13-x}\text{B}_x$  is that it is unchanged by the superconducting transition and that, within experimental error, it is the same for  $x=0.067$  and  $0.030$ . This temperature independence has been observed in some uranium-based heavy-fermion superconductors, but not in others. For example, a temperature-independent NMR shift in the superconducting state has been reported for  $\text{U}_{0.967}\text{Th}_{0.033}\text{Be}_{13}$  (Ref. 8) and  $\text{UPt}_3$ .<sup>39</sup> On the other hand, a reduction of 20% has been reported for  $\text{UPd}_2\text{Al}_3$  (Ref. 40) and  $\mu\text{SR}$  results have indicated a reduction of 10–40% for  $\text{UBe}_{13}$ .<sup>41</sup> (We are unaware of any superconducting NMR Knight shift studies in undoped  $\text{UBe}_{13}$ .) In no case is the full vanishing Knight shift of the Yosida model<sup>29</sup> observed.

It is natural to assume that this behavior of  $K_B$  is the result of a temperature-independent spin susceptibility. A finite spin susceptibility at zero temperature can originate from a variety of mechanisms. They include spin-orbit scattering,<sup>42</sup> gapless superconductivity, and spin-triplet pairing of the Cooper pairs.<sup>43</sup> We attribute strong spin-orbit scattering as the dominant mechanism for the temperature independence of  $K_B$ . Although the  $1/T_1$  data indicate the occurrence of a gapless superconducting state with B doping, it does not appear to be the most important contribution. If the DOS of the gapless states were large enough to cause the temperature independence of  $K_B$ , we would expect  $K_B$  to be substantially larger for  $x=0.067$  than for  $x=0.030$ , but they are the same within uncertainties. Since there is no other conclusive evidence of spin-triplet Cooper pairing in these materials, we reject this possibility as a mechanism for the behavior of  $K_B$ .

## V. CONCLUSIONS

The NMR results in this study provide insight into how the magnetic response and the superconducting DOS are modified when B is doped into  $\text{UBe}_{13}$ . In the normal state, above  $\sim 4$  K,  $1/T_1$  values for  $^9\text{Be}$  or  $^{11}\text{B}$  for all B concentra-

tions are indistinguishable within experimental uncertainties. At lower temperatures, of the order of 1 K, significant differences exist, with  $x=0.067$  having a  $1/T_1$  roughly twice that compared to the  $x=0.030$  sample for both nuclei. The  $x=0.030$  sample has essentially the same  $1/T_1$  magnitude and temperature dependence as undoped  $\text{UBe}_{13}$ . For a span of about 1–2 K above  $T_c$ , the temperature dependence for the  $x=0.030$  sample shows a Korringa-like dependence. In the  $x=0.067$  sample, deviations from this behavior are observed, possibly reflecting a reduction in  $T^*$ . Below  $\sim 1$  K,  $1/T_1 T$  exhibits a monotonic decrease in both sample concentrations. The  $^{11}\text{B}$  hyperfine field coupling constant, extracted from the linear plot of  $K_B$  versus  $\chi$ , was calculated to be  $-361.1$  Oe/ $\mu_B$ .

Using an approximate analysis of the U moment electronic fluctuation rate, we observe a  $\Gamma \propto \sqrt{T}$  dependence in a temperature range between 8 and 70 K, which is consistent with the existence of isolated local moment fluctuations at high temperatures. For  $T > 70$  K, the  $\Gamma$  analysis breaks down due to the presence of crystal field excitations. Measurements of  $1/T_1$  indicate a moderate decrease in  $\Gamma$  with the addition of boron at low temperatures, where  $\Gamma(x=0.030)/\Gamma(x=0.067) \sim 2$ . At lower temperatures,  $\Gamma$  approaches a constant value of the order of 1 meV near 2 K. This value is comparable to the magnitude of the renormalized density of states obtained from thermodynamic measurements and for  $x=0.030$  compares favorably with quasi-elastic neutron scattering experiments in the undoped material.

In the superconducting state, we investigated the  $T$  dependence of  $T_1$  for both the  $^9\text{Be}$  and  $^{11}\text{B}$  nuclei. Below  $T_c$ ,  $1/T_1$  exhibited a strong B concentration dependence, especially at the lowest temperatures. We interpret this behavior as consistent with gapless superconductivity induced by the B impurities. Due to the small amount of B dopant, we speculate that the B impurities act like strong scattering centers near the unitary limit. This hypothesis is supported by semiquantitative agreement of our low-temperature  $T_1$  results with theoretical predictions for resonant impurity scattering in anisotropic superconductors. The ratio of the  $^9\text{Be}$  to  $^{11}\text{B}$   $1/T_1$  increased with decreasing temperature below  $T_c$ . This observation indicates that additional contributions to the  $^9\text{Be}$  relaxation rate are present at low temperatures. We attribute this effect to spin diffusion processes that have little impact on the dilute  $^{11}\text{B}$ ; thus the  $^{11}\text{B}$   $T_1$  results may more accurately reflect the intrinsic quasiparticle relaxation compared to the  $^9\text{Be}$ . Below  $T_c$ , the  $^{11}\text{B}$  Knight shift was measured to be  $-0.08$  ( $\pm 0.01$ )%. This value is independent of  $x$  and  $T$  within our experimental uncertainties and is presumably due to strong spin-orbit scattering in these materials.

## ACKNOWLEDGMENTS

We thank D. E. MacLaughlin, M. Takigawa, A. V. Balatsky, and W. P. Beyermann for enlightening discussions. One of us (E.T.A.) acknowledges support from the Associated Western Universities for much of this work. This work was funded in part by NSF Grant No. DMR-9705369. Work at Los Alamos was performed under the auspices of the U.S. Department of Energy.

- \* Author to whom correspondence should be addressed. Present address: Beckman Institute and Division of Biology, California Institute of Technology, MS 139-74, Pasadena, CA 91125. FAX: (626) 449-5163. Electronic address: eta@gg.caltech.edu
- <sup>†</sup> Present address: National High Magnetic Field Laboratory, Florida State University, 1800 Paul Dirac Drive, Tallahassee, FL 32310.
- <sup>1</sup> A. L. Giorgi, Z. Fisk, J. O. Willis, G. R. Stewart, and J. L. Smith, in *Proceedings of the 17th International Conference on Low Temperature Physics, LT-17*, edited by U. Eckern, A. Schmid, W. Weber, and H. Wuhl (North-Holland, Amsterdam, 1984), p. 229.
- <sup>2</sup> H. R. Ott, H. Rudigier, Z. Fisk, and J. L. Smith, *Phys. Rev. B* **31**, 1651 (1985); R. H. Heffner, J. L. Smith, J. O. Willis, P. Birrer, C. Baines, F. N. Gygax, B. Hitti, E. Lippelt, H. R. Ott, A. Schenck, E. A. Knetsch, J. A. Mydosh, and D. E. MacLaughlin, *Phys. Rev. Lett.* **65**, 2816 (1990).
- <sup>3</sup> Z. Fisk and H. R. Ott, *Int. J. Mod. Phys. B* **3**, 535 (1989); E. Felder, A. Bernasconi, H. R. Ott, Z. Fisk, and J. L. Smith, *Physica C* **162-164**, 429 (1989); H. R. Ott, E. Felder, Z. Fisk, R. H. Heffner, and J. L. Smith, *Phys. Rev. B* **44**, 7081 (1991).
- <sup>4</sup>  $T^*$  is defined as the temperature where the entropy  $\Delta S$  reaches a value given by  $\Delta S = \int_0^{T^*} \gamma dT = R \ln 2$  per mole of actinide (fully compensated moment), where  $\gamma$  is the electronic heat capacity.
- <sup>5</sup> W. P. Beyermann, R. H. Heffner, J. L. Smith, M. F. Hundley, P. C. Canfield, and J. D. Thompson, *Phys. Rev. B* **51**, 404 (1995).
- <sup>6</sup> E. T. Ahrens, P. C. Hammel, R. H. Heffner, A. P. Reyes, J. L. Smith, and W. G. Clark, *Phys. Rev. B* **48**, 6691 (1993).
- <sup>7</sup> E. T. Ahrens, R. H. Heffner, P. C. Hammel, A. P. Reyes, and J. L. Smith, *Physica B* **206&207**, 589 (1995).
- <sup>8</sup> D. E. MacLaughlin, Cheng Tien, W. G. Clark, M. D. Lan, Z. Fisk, J. L. Smith, and H. R. Ott, *Phys. Rev. Lett.* **53**, 1833 (1984).
- <sup>9</sup> N. E. Alekseevskii and E. G. Nikolaev, *Sov. Phys. JETP* **64**, 1078 (1987).
- <sup>10</sup> W. G. Clark, M. C. Lan, G. van Kalker, W. H. Wong, Cheng Tien, D. E. MacLaughlin, J. L. Smith, Z. Fisk, and H. R. Ott, *J. Magn. Magn. Mater.* **63-64**, 396 (1987).
- <sup>11</sup> W. G. Clark, W. H. Wong, W. A. Hines, M. D. Lan, D. E. MacLaughlin, Z. Fisk, J. L. Smith, and H. R. Ott, *J. Appl. Phys.* **63**, 3890 (1988).
- <sup>12</sup> M. Benakki, A. Qachaou, and P. Panissod, *J. Magn. Magn. Mater.* **73**, 141 (1988).
- <sup>13</sup> R. E. Walstedt, E. L. Hahn, C. Froidevaux, and E. Geissler, *Proc. R. Soc. London, Ser. A* **284**, 499 (1965); M. I. Aalto, H. K. Collan, R. G. Gylling, and K. O. Nores, *Rev. Sci. Instrum.* **44**, 1075 (1973).
- <sup>14</sup> E. Fukushima and S. B. W. Roeder, *Experimental Pulse NMR: A Nuts and Bolts Approach* (Addison-Wesley, Reading, MA, 1981).
- <sup>15</sup> J. M. Moore, W. G. Clark, and W. H. Wong, *Phys. Rev. B* **38**, 11 163 (1998).
- <sup>16</sup> *Metallic Shifts in NMR*, edited by G. C. Carter, L. H. Bennet, and D. J. Kahan (Pergamon, Oxford, 1978).
- <sup>17</sup> G. Remenyi, D. Jaccard, J. Flouquet, A. Briggs, Z. Fisk, J. L. Smith, and H. R. Ott, *J. Phys. (Paris)* **47**, 367 (1986).
- <sup>18</sup> E. T. Ahrens, Ph.D. thesis, University of California at Los Angeles, 1994.
- <sup>19</sup> H. M. Mayer, U. Rauchschalbe, C. D. Bredl, F. Steglich, H. Rietschel, H. Schmidt, H. Wuhl, and J. Beuers, *Phys. Rev. B* **33**, 3168 (1986).
- <sup>20</sup> D. Einzel, P. J. Hirschfeld, F. Gross, B. S. Chandrasekhar, K. Andres, H. R. Ott, J. Beuers, Z. Fisk, and J. L. Smith, *Phys. Rev. Lett.* **56**, 2513 (1986).
- <sup>21</sup> W. G. Clark (unpublished).
- <sup>22</sup> A. Narath, *CRC Crit. Rev. Solid State Sci.* **3**, 1 (1972).
- <sup>23</sup> D. L. Cox, *Phys. Rev. B* **35**, 6504 (1987).
- <sup>24</sup> A. Qachaou, E. Beaupaire, M. Benakki, B. Lemius, J. P. Kappler, A. J. P. Meyer, and P. Panissod, *J. Magn. Magn. Mater.* **63-64**, 635 (1987); M. Benakki, J. P. Kappler, and P. Panissod, *J. Phys. Soc. Jpn.* **56**, 3309 (1987).
- <sup>25</sup> D. L. Cox, N. E. Bickers, and J. W. Wilkins, *J. Appl. Phys.* **57**, 3166 (1985).
- <sup>26</sup> G. H. Lander, S. M. Shapiro, C. Vettier, and A. J. Dianoux, *Phys. Rev. B* **46**, 5387 (1992).
- <sup>27</sup> Z. Fisk, D. W. Hess, C. J. Pethick, D. Pines, J. L. Smith, J. D. Thompson, and J. O. Willis, *Science* **239**, 33 (1988).
- <sup>28</sup> A. I. Goldman, S. M. Shapiro, G. Shirane, J. L. Smith, and Z. Fisk, *Phys. Rev. B* **33**, 1627 (1986).
- <sup>29</sup> D. E. MacLaughlin, *Solid State Phys.* **31**, 1 (1976).
- <sup>30</sup> J. M. Moore, Ph.D. thesis, University of California at Los Angeles, 1991.
- <sup>31</sup> D. E. MacLaughlin, M. D. Lan, C. Tien, J. M. Moore, W. G. Clark, Z. Fisk, J. L. Smith, and H. R. Ott, *J. Magn. Magn. Mater.* **63-64**, 455 (1987).
- <sup>32</sup> P. W. Anderson, *J. Phys. Chem. Solids* **11**, 26 (1959).
- <sup>33</sup> A. A. Abrikosov and L. P. Gor'kov, *Sov. Phys. JETP* **12**, 1243 (1961).
- <sup>34</sup> P. J. Hirschfeld, D. Vollhardt, and P. Wolfle, *Solid State Commun.* **59**, 111 (1986); P. J. Hirschfeld, P. Wolfle, and D. Einzel, *Phys. Rev. B* **37**, 83 (1988).
- <sup>35</sup> C. J. Pethick and D. Pines, *Phys. Rev. Lett.* **57**, 118 (1986); S. Schmitt-Rink, K. Miyake, and C. M. Varma, *ibid.* **57**, 2575 (1986).
- <sup>36</sup> K. Ishida, Y. Kitaoka, N. Ogata, T. Kamino, K. Asayama, J. R. Cooper, and N. Athanassopoulou, *J. Phys. Soc. Jpn.* **62**, 2803 (1993); M. Takigawa and D. B. Mitzi, *Phys. Rev. Lett.* **73**, 1287 (1994).
- <sup>37</sup> A. V. Balatsky, P. Monthoux, and D. Pines, *Phys. Rev. B* **50**, 582 (1994).
- <sup>38</sup> D. S. Jin, T. F. Rosenbaum, J. S. Kim, and G. R. Stewart, *Phys. Rev. B* **49**, 1540 (1994).
- <sup>39</sup> Y. Kohori, T. Kohara, H. Shibai, Y. Oda, Y. Kitaoka, and K. Asayama, *J. Phys. Soc. Jpn.* **56**, 2263 (1987).
- <sup>40</sup> M. Kyogaku, Y. Kitaoka, K. Asayama, N. Sato, T. Sakon, T. Komatsubara, C. Geibel, C. Shank, and F. Steglich, *Physica B* **186-188**, 285 (1993).
- <sup>41</sup> R. H. Heffner, D. W. Cooke, Z. Fisk, R. L. Hutson, M. E. Schillaci, J. L. Smith, J. O. Willis, D. E. MacLaughlin, C. Boekema, R. L. Lichti, A. B. Denison, and J. Oostens, *Phys. Rev. Lett.* **57**, 1255 (1986).
- <sup>42</sup> R. A. Ferrell, *Phys. Rev. Lett.* **3**, 262 (1959); P. W. Anderson, *ibid.* **3**, 325 (1959).
- <sup>43</sup> A. J. Leggett, *Rev. Mod. Phys.* **47**, 331 (1975).